Post-Eruptive Arcade Formation in the 25 January 2007 CME/Flare Limb Event: Microwave Observations with the RATAN-600 Radio Telescope

I.Y. Grigoryeva · V.N. Borovik · M.A. Livshits · V.E. Abramov-Maximov · L.V. Opeikina · V.M. Bogod · A.N. Korzhavin

Abstract A CME/flare event occurred at the eastern limb on 25 January, 2007. Seven successive multi-wavelength scans in the range 1.8 cm – 5.0 cm were obtained with the RATAN-600 radio telescope starting just at the beginning of the post-eruptive arcade formation (30 min after a C6.3 flare peak) and lasting for 3.5 hours. The conditions were favorable to study the off-limb microwave radio source associated with the post-eruptive arcade in different phases of its formation. Microwave radio emission of the arcade was rather intense initially and then considerably decreased; its maximum was co-spatial with the 195 Å Fe XII loop tops. The RATAN-600 total flux spectra of the off-limb radio source were practically flat during the first two hours indicating a predominant contribution of thermal emission. The X-ray spectrum was thermal (according to RHESSI data) at that time. Data available in the meter wavelength range during this phase were indicative of weak non-thermal processes likely due to accelerated particles. However, free – free emission of an isothermal source dominated in microwaves. This is indicative of the presence of a large amount of plasma in the region of arcade formation at the initial stage of the event. The weak microwave emission during the decay phase might be interpreted as the thermal cyclotron emission of the loops in the arcade.

Keywords Coronal mass ejections, initiation and propagation · Flares, energetic particles

I.Y. Grigoryeva · V.N. Borovik (✉) · V.E. Abramov-Maximov
Central Astronomical Observatory at Pulkovo, Russian Acad. Sci., St. Petersburg, Russia
e-mail: vnborovik@mail.ru

M.A. Livshits
Pushkov Institute of Terrestrial Magnetism, Ionosphere and Radiowave Propagation of Russian Acad. Sci., Troitsk, Russia

L.V. Opeikina
Special Astrophysical Observatory of Russian Acad. Sci., Nizhni Arkhyz, Russia

V.M. Bogod · A.N. Korzhavin
Saint-Petersburgs Branch of SAO RAS, St. Petersburg, Russia

1. Introduction

When studying non-stationary solar phenomena, coronal mass ejections (CME) and the associated flares are considered as two parts of the same event. The main features of a solar eruptive event are determined by the magnetic configuration and velocity field. The relation between an ejection (jet or CME) and the flare itself is rather complicated and now it is being widely studied. CMEs have been observed for 30 years with a variety of instruments. It is now possible to derive detailed and quantitative information on CME morphology, velocity, acceleration and mass. Flares associated with CMEs are observed in X-rays, and several different radio signatures are also present. Optical and UV spectra of CMEs both on the disk and at the limb provide velocities along the line of sight and diagnostics for temperature, density, and composition (see, *e.g.*, Schwenn *et al.*, 2006).

According to the standard scenario of an eruptive flare, sometimes referred to as "CSHKP" for its main contributors (Carmichael, 1964; Sturrock, 1966; Hirayama, 1974; Kopp and Pneuman, 1976), a set of magnetic field lines "open", *i.e.* expand during the eruption. Later some "open" field lines close down due to a reconnection process in the current sheet in the wake of the eruption. Then, the loops located below the current sheet shrink while plasma above the current sheet is thrown out into the interplanetary space. The ascending loop system observed after powerful eruptive events is the result of successive magnetic field reconnections in the corona.

Many important results concerning the relationship between flares and CMEs and development of the models of non-stationary solar processes have been obtained in the studying of the CME/flare events (1996 – 2005) (see, *e.g.*, Yashiro *et al.*, 2008) using data of the Large Angle and Spectrometric Coronagraph (LASCO) on board the *Solar and Heliospheric Observatory* (SOHO). A detailed analysis of the powerful geo-effective solar events in the period of October – November 2003 was made by Gopalswamy *et al.* (2005a, 2005b).

The role of plasma ejections in the development of major solar flares of various durations has been considered by several authors (see, *e.g.*, Gary and Moore, 2004; Harra *et al.*, 2005; Shakhovskaya, Livshits, and Chertok, 2006). It was shown that wide ejections and bright large-scale CMEs usually are accompanied by the formation and existence of a long-duration extended arch system.

Formerly postflare loops were observed in Hα line and in soft X-rays (SXR) by spaceborne observations (*Yohkoh*/SXT). Now, when dynamic flares occur, they are well detected also in extreme ultraviolet (EUV) with EUV Imaging Telescope (EIT) on board SOHO and the *Transition Region and Coronal Explorer* (TRACE) in 195 Å Fe XII and in other ranges. For example, the development of the X1.5 flare on 21 April 2002, and its different posteruptive manifestations were studied by Kundu *et al.* (2004) as well as by other authors (see, *e.g.*, Gallagher *et al.*, 2002; Sheeley, Warren, and Wang, 2004; Chernov, 2006), using microwaves at the Nobeyama Radioheliograph, and the spectropolarimeter of the Huairou station (China) and hard X-ray images at the *Reuven Ramaty High-Energy Solar Spectroscopic Imager* (RHESSI).

Long lived microwave radio sources (some of them being off-limb at a height of up to 170 000 km) were reported about two decades ago. A coronal radiation source related to a Hα prominence was first noted by Kundu (1972). Later, many limb microwave sources observed during 1979 – 1983 were studied in more detail by other authors (see, *e.g.*, Urpo, Krüger, and Hildebrandt, 1986; Urpo *et al.*, 1989; Borovik *et al.*, 1989; Krüger *et al.*, 1994). These sources were related to postflare manifestations, but, because no regular soft X-ray observations were available at that time, they could not be directly identified with posteruptive arcades. In the last years those long-lived coronal formations were studied using

multi-spectral data and radio astronomy methods. Analyses of post-eruptive arcades observed in various spectral domains have been addressed in several papers (see, *e.g.*, Ichimoto and Sakurai, 1994; Feldman *et al.*, 1995; Harra-Murnion *et al.*, 1998; Altyntzev *et al.*, 1999; Kamio, Kurokawa, and Ishi, 2003; Grechnev *et al.*, 2004). New important information on plasma parameters in the post-eruptive arcades has been obtained by the telescope SPIRIT on board CORONAS-F, especially in Mg XII 8.42 Å (reported briefly for the first time by Zhitnik *et al.*, 2003).

Using CORONAS-F/SPIRIT data, we previously analyzed post-eruptive arcades observed after eruptive phenomena (one or more CMEs) on 22 October 2001, 12 November 2001, and 28–29 December 2001 (Grechnev *et al.*, 2006a, 2006b; Borovik *et al.*, 2007). The related flares had different power and belonged to different X-ray classes, namely: the 22 October 2001, flare was an M1.0, the 12 November 2001, a C7.0, the 28 December 2001, an X4.0. The arcades in these events were observed late at the post-eruptive stages, 6–12 hours after the peak of the related flare. Plasma parameters in the post-eruptive arcades turned out to be the following: the temperature in the microwave and SXR sources was 5–10 MK, and the electron density was $(5-10) \times 10^9$ cm^{-3}. The observational results indicated a prolonged energy release high in the corona in the form of heating that could maintain high temperatures in the arcades, with the highest values at their tops. The microwave observations made during these events at the Nobeyama Radioheliograph (NoRH), at the Siberian Solar Radio Telescope (SSRT), and at the RATAN-600 radio telescope showed that the radio emission of post-eruptive arcades contained a non-thermal component, which was indicative of the presence of accelerated particles.

Unlike the previously studied events related to flares of the M or X GOES classes, we tried to observe with the RATAN-600 the formation of a post-eruptive arcade in a weaker event (not exceeding the GOES class C). One might expect the contribution of the accelerated particles to the microwave emission to be minimal in such events thus enabling one to study plasma parameters in post-eruptive arcades. It was the 25 January 2007 event during which we succeeded to observe with RATAN-600 a post-eruptive arcade starting from the onset of its formation.

In this paper we present the observations made with the RATAN-600 radio telescope during the initial stage of the post-eruptive arcade formation in the CME/flare limb event on 25 January 2007. Section 2 describes observations carried out at the RATAN-600 radio telescope. Section 3 is devoted to the description of the CME/flare limb event and the related phenomena in different ranges. The discussion and some conclusions are given in Section 4.

2. RATAN-600 data

In January 2007 solar observations were carried out daily at the reflector-type radio telescope RATAN-600 (Korol'kov and Parijskij, 1979) in the celestial meridian and six azimuths at different positional angles (one observation was at the local noon, three before noon and three after noon) with time intervals of about 35 min. South sector of main mirror and flat periscope mirror were used in these observations. The knife-like diagram pattern of the radio telescope (FWHM) in this case was determined by the following relations: $\Theta_{\text{horizontal}}$(arc sec) $= 8.5 \times \lambda$ (cm), Θ_{vertical}(arc min) $= 6.5 \times \lambda$ (cm). Right and left circularly polarized components (RCP and LCP) were recorded at 44 wavelengths simultaneously within the wavelength range of 1.8–5.0 cm, while the Sun crossed the fixed antenna array. The total intensity (Stokes parameter "I") and the circularly polarized component (Stokes parameter "V") are calculated as $I = \text{RCP} + \text{LCP}$ and $V = \text{RCP} - \text{LCP}$.
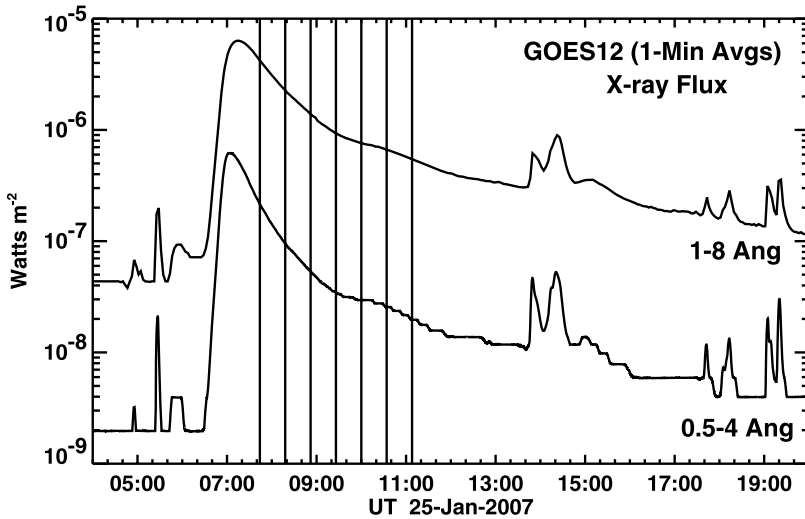
Figure 1 GOES plot of 1 minute averages of the solar soft X-ray flux output in the $1-8$ Å and $0.5-4$ Å passbands for 25 January 2007. Vertical lines show the times of RATAN-600 observations.

On 25 January, the solar observations were made at 07:44, 08:18, 08:52, 9:26 (local noon), 10:00, 10:34, and 11:08 UT. These times are marked in Figure 1 with vertical lines. The weak flare GOES class C3.6 occurred in the NOAA AR 10940 behind the east limb. The first observation was made 30 min after the flare peak. The angles of the knife-like antenna diagram measured from the solar axis to the different azimuths were $-0.2°$, $-3.4°$, $-6.3°$, $-9.0°$, $-11.8°$, $-14.7°$, $-17.9°$ (from the earliest azimuth to the latest one respectively). A method of multi-azimuth solar observations on the RATAN-600 radio telescope is considered by Nindos *et al.* (1996).

Emission in the microwave range of active region NOAA AR 10940 (the most likely source region of the CME), situated behind the east limb on 25 January was recorded on the next day. This circumstance provided favorable conditions to study the microwave emission from the post-eruptive arcade, associated with eruptive event on the east limb.

Figures 2(a – g) show, as an example, one-dimensional RATAN-600 solar scans (Stokes "*I*") at 2.9 cm obtained in different azimuths. In Figure 2(d), the solar scan is overlaid on a SOHO/EIT 195 Å Fe XII image (reversed intensity). The orientation of the solar image was changed to fit the RATAN-600 observations. The scans show an off-limb radio source on the east associated with the post-eruptive arcade and another one, on the west limb, associated with active region NOAA AR 10939. The co-alignment error between the scan and the 195 Å image is assumed to be of 5 arc sec. We used the radio sources (in "*I*" and "*V*" channels) associated with bright points in the 195 Å image and the leader sunspot of NOAA AR 10939 for the co-alignment. It is well seen that the intensity of the off-limb radio source decreased considerably with time.

In Figure 2(h) we show a portion of the scan (Stokes parameters "*I*" and "*V*") in the shortest wavelength (1.8 cm) at 09:26 UT; this portion is close to the east solar limb, which is marked with a dashed line. We can see two components of the off-limb radio source (shown by arrows) which could be resolved due to the higher spatial resolution of the antenna at this wavelength.
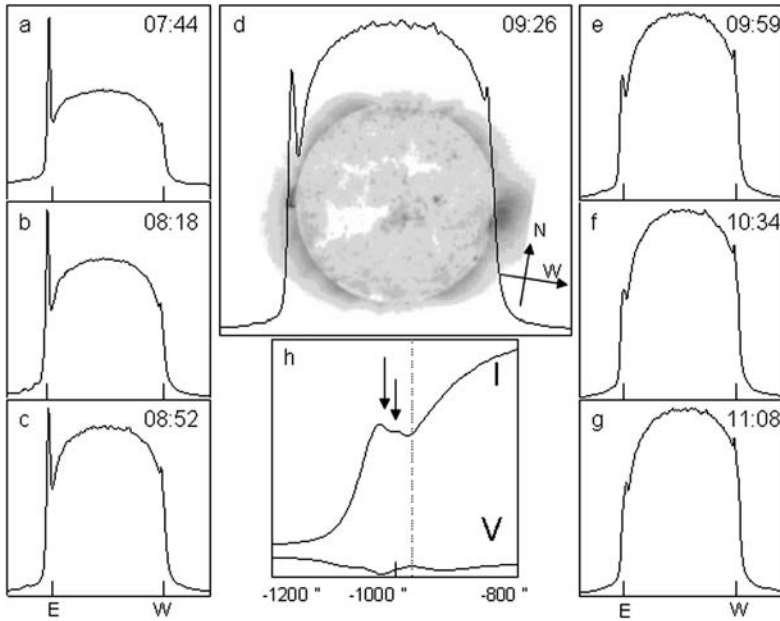
Figure 2 One-dimensional RATAN-600 solar scans (Stokes "*I*") at 2.9 cm, obtained in different azimuths (a – c, e – g). One-dimensional RATAN-600 solar scan (Stokes "*I*") at 3 cm at 09:26 UT overlaid on the SOHO/EIT 195 Å Fe XII image at 09:24 UT (d). The cross with arrows in the right bottom corner shows N – S and E – W directions on the solar disk. (h) The east part of the solar scans at the wavelength 1.8 cm ("*I*" and "*V*") at 09:26 UT. Arrows show two components of the off-limb radio source. Dashed line shows the solar limb.

The RATAN-600 data have two major advantages: a very high sensitivity in flux measurements (several mJy) due to the huge effective area of the antenna system, and multi-frequency observations in a wide microwave range. At the same time, there are two disadvantages: the ambiguity of the one-dimensional data and the instrumental polarization contribution at the solar limb due to the specific antenna configuration. To extract reliably the off-limb source in the solar scans obtained on 25 January, we used the scans of the previous day (24 January), when neither on-limb, nor off-limb radio sources were present near the east limb.

In Figures 3(a – f), one can see a sequence of off-limb radio sources (given in arbitrary units) extracted from the scans at 2.9 cm in channel "*I*" and in channels "*I*" and "*V*" (Figure 3(g)) overlaid on the post-eruptive arcade reversed intensity images (195 Å SOHO/EIT). Solid lines under the radio sources show the direction of the Sun scanning in the RATAN-600 observations.

The evolution of the post-eruptive arcade in 195 Å can be seen in Figure 3 as well as in Figure 4. The orientation of the solar image in Figure 4 was changed to fit RATAN-600 observations. In Figure 4, the vertical solid lines show the locations of peak intensity of the off-limb radio source and the dotted vertical lines show the location of the second component of the radio source (when it could be resolved). Images of the arcade (195 Å SOHO/EIT) are shown at times closest to those of the RATAN-600 observations. A bright diffuse source can be seen close to the east limb (at 07:36 and 07:48 UT). The first loop system (labeled as "1") is seen in the next RATAN-600 observation at 08:18 UT (Figure 4(c)). According to 195 Å images (Figures 4(c – h)) the height in plane-of-the-sky of loop system "1" changed
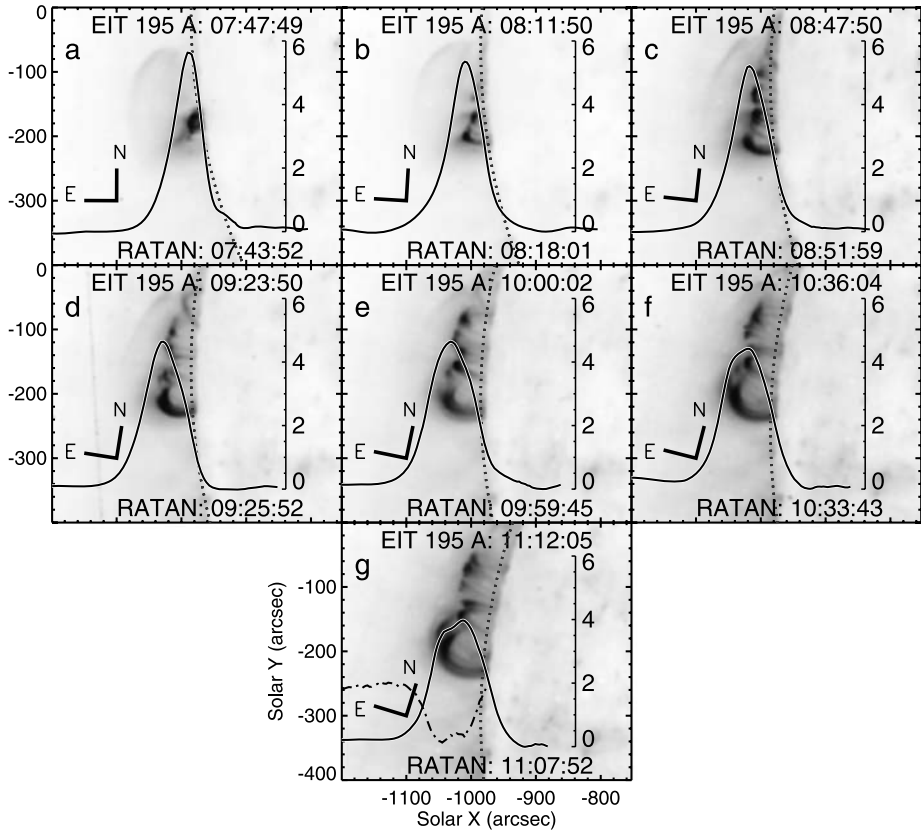
Figure 3 Sequence of off-limb radio observations (in arbitrary units, right scale) extracted from RATAN-600 scans at 2.9 cm in channel "*I*" (a – f) and in channels "*I*" and "*V*" (g) overlaid on the post-eruptive arcade reversed intensity images (195 Å SOHO/EIT). Axes show arc seconds from the solar disk center.

from 25 000 km at 08:12 UT to 35 000 km at 09:24 UT and to 50 000 km at 11:12 UT. The apparent ascending velocity in this time interval was practically constant, 2.3 km s^{-1}. The 195 Å images obtained by SOHO/EIT after 11:12 UT show that this velocity decreased. This agrees with the evolution of Hα and SXR postflare loops, *e.g.*, in the well studied limb event of 2 November 1992 (Harra-Murnion *et al.*, 1998; Kamio, Kurokawa, and Ishi, 2003). Other loop systems (labeled as "2" and "3") appeared northward and developed as time went on (Figures 4(d – h)). Figure 4 shows that in all RATAN-600 observations the maxima of intensity of the microwave emission (solid vertical lines) are positioned on the tops of 195 Å arcades. From the latest RATAN-600 observations, we observe that the locations of a second component of the off-limb radio source, when it is resolved (shown by dotted lines), coincides with the upper part of a new "northern" loop system labeled as "2" and "3" in (Figures 4(d – h)).

It should be noted that it is difficult to reliably estimate the intensity and effective sizes of the two radio source components. However, it can be concluded from the two latest RATAN-600 observations that the microwave emission from the northern (new) loop system ("3") is more intense than that from the southern (old) one ("1"). At the same time, the radio

Figure 4 Sequence of 195 Å images of the post-eruptive arcade on 25 January 2007, obtained at times close to RATAN-600 observations. Solar images are rotated so that the Sun scanning direction on RATAN-600 is horizontal. Vertical solid lines show the locations of peak intensity of the off-limb radio source and the dotted vertical lines show the location of the second component of the radio source (when it could be resolved). The solar limb in the optical range is shown with a dashed line. The horizontal segments at the bottom of the figures show the effective sizes of the off-limb radio sources. The crosses in the lower right corners show N – S and E – W directions on the solar disk. "1", "2" and "3" correspond to the loop systems described in the text.
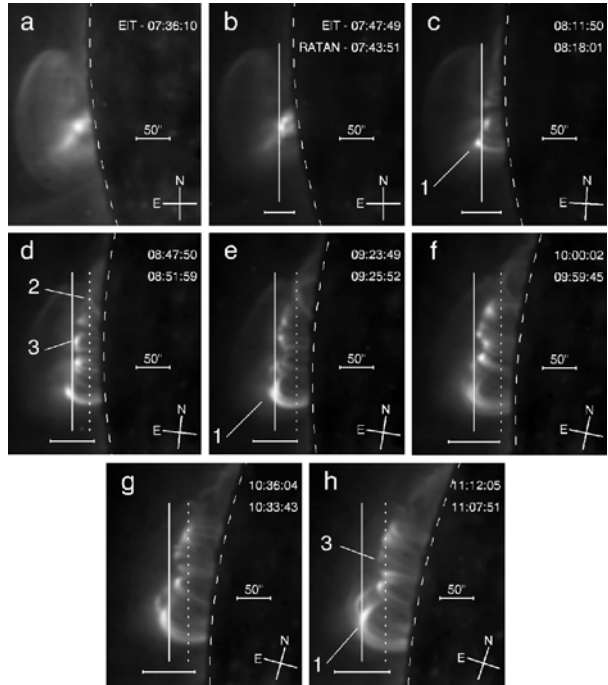
emission of the "old" loop system is more polarized (the degree of circular polarization is about 12%) than that of the "new" one. Figure 3(g) confirms this fact.

Here we concentrate on the global characteristics of the off-limb microwave radio source associated with the whole post-eruptive arcade and its evolution during the arcade formation.

We estimated the one-dimensional effective (deconvolved) size "D" of the microwave-emitting region along the scanning direction as $D = (A^2 - B^2)^{1/2}$ with A and B being the FWHMs of the source scan and RATAN-600 beam width, respectively. Gaussian shapes for both the one-dimensional brightness distribution over the "real" radio source and the beam were assumed herewith.

The effective sizes of the radio source at all wavelengths in the operating range of 1.8 – 5.0 cm turned out to be practically the same. Averages over all wavelengths for the effective size D (r.m.s. < 10 %) obtained from seven observations with RATAN-600 are listed in Table 1.

The sizes D are shown in Figures 4(b – h) with horizontal segments under the arcade. In the first observation the effective size of the microwave-emitting region is larger than that of the small loop in 195 Å at the limb. In the later observations the radio sizes are found to be approximately the same as the projections of the whole loop system on the scanning direction.

Under the assumption of a Gaussian profile for the source, its brightness temperature T_b was estimated as

$$T_b(\text{K}) = 5.45 \times 10^3 S \lambda^2 D^{-2},$$

where S is the flux density (sfu), λ is the wavelength (cm), D is the deconvolved size of the radio source (arc min). The parameters of the off-limb radio source estimated from seven RATAN-600 observations are listed in Table 1: the flux densities S at the shortest

Figure 5 Total flux microwave spectra of the off-limb radio source associated with a post-eruptive arcade for different times of RATAN-600 observations.
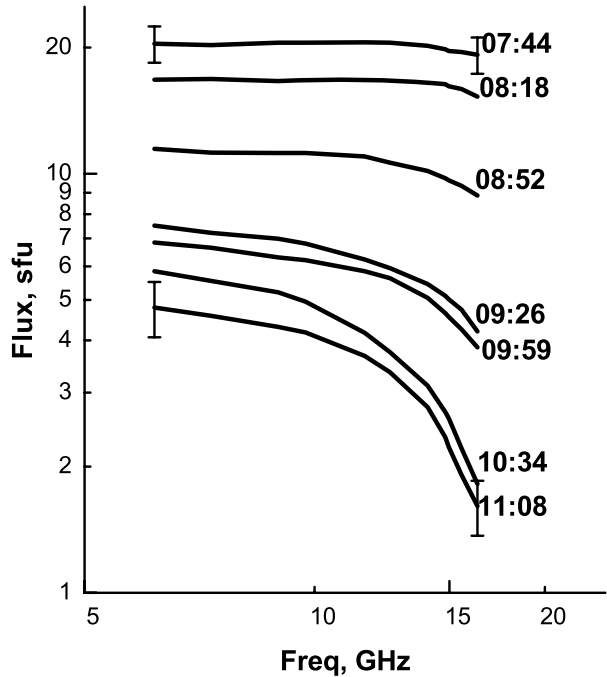
Table 1 Radio flux density S, effective size D and effective brightness temperature T_b of the off-limb radio source at 1.8 and 5 cm.

Time, UT	S, sfu		D, arc sec	T_b, MK	
	1.8 cm	5.0 cm		1.8 cm	5.0 cm
07:43:51	19.2	20.3	44	0.64	5.2
08:18:01	14.6	16.4	58	0.27	2.4
08:51:59	8.9	11.2	64	0.14	1.3
09:25:52	4.2	7.9	66	0.06	0.9
09:59:45	3.6	6.8	77	0.04	0.6
10:33:43	1.8	5.9	76	0.02	0.5
11:07:51	1.6	4.8	82	0.01	0.35

(1.8 cm) and longest (5.0 cm) wavelengths, the effective (averaged over all wavelengths in the operating range) deconvolved size D and the effective brightness temperature T_b at 1.8 cm and 5.0 cm.

The evolution of the total flux spectra of the off-limb radio source associated with the post-eruptive arcade can be seen in Figure 5. The spectra are constructed as the upper envelope of spectra obtained by using all wavelengths in the operating range. The error in the flux measurements (10 – 15 %) is determined by the accuracy of both the separation of the off-limb source and the calibration technique. For absolute calibration we used the Moon and Crab Nebula observations made with the RATAN-600 radio telescope. The total fluxes in microwaves measured at different solar stations (Nobeyama, Pentincton, Learmonth) were also taken into account.

Figure 5 shows the microwave spectrum to be practically flat at the early formation of the post-eruptive arcade. This suggests that the thermal emission predominated immediately

after the flare maximum. This conclusion drawn from the emission integrated over the whole source is certainly restricted to more or less uniform source. The fluxes decreased later on for several hours, especially at the highest frequencies.

Considering that thermal bremsstrahlung was the predominant mechanism for microwave emission at the early stages of the arcade formation, we can estimate the emission measure (EM) using the well-known expression for an optically thin plasma:

$$S(\text{sfu}) \sim 3 \times 10^{-45} \text{EM}(\text{cm}^{-3}) T(\text{K})^{-1/2},$$

where S is the total radio flux and T is the temperature of the emitting plasma.

Taking the flux S at shortest wavelength (1.8 cm) and assuming that the brightness temperature at the longest wavelength (5.0 cm) is the lowest limit of the kinetic plasma temperature in the arcade, because $\tau(5 \text{ cm}) \gg \tau(1.8 \text{ cm})$ (τ is the optical thickness), we obtain EM $= 14.6 \times 10^{48}$ cm^{-3} at 07:44 UT and EM $= 7.5 \times 10^{48}$ cm^{-3} at 08:18 UT.

Assuming the volume of the emission region as $V = D^3$, where D is the effective size of the radio source, we get the average electron density 2.2×10^{10} cm^{-3} and 1.0×10^{10} cm^{-3}, respectively.

One should note that the effective sizes of the microwave source at different positional angles did not change significantly. This fact probably indicates that this source is rather compact. The results under consideration obtained three hours after the flare peak are in agreement with those of the post-eruptive arcade at the late stage of the eruptive event on 22 October 2001 (Grechnev *et al.*, 2006a, 2006b), which supports this conclusion. The arcade on 22 October 2001 was observed with CORONAS-F/SPIRIT, *Yohkoh*/SXT, SOHO/EIT and in microwaves. Figures 1 and 2 in Grechnev *et al.* (2006b) show an overlay of various images of the arcade in different wavelengths. A corresponding compact source is reliably detected in the emission of plasmas with temperatures of $0.1 - 10$ MK. Note that previous multi-wavelength analyses of post-eruptive arcades revealed large upward temperature gradients (Harra-Murnion *et al.*, 1998; Kamio, Kurokawa, and Ishi, 2003).

3. Results of Multi-Wavelength Observations of the Event on 25 January 2007

In this section we briefly discuss some features of the event derived from multi-wavelength observations which are useful for understanding the CME/flare event.

According to the NOAA Space and Environment Center, the beginning of the related flare C6.3 (GOES class) was at 06:33 UT, the end at 07:58 UT, and the flare peak at 07:14 UT. First, we consider X-ray observations. RHESSI observed the event along two intervals: $06:33 - 07:10$ UT and $07:45 - 08:45$ UT. Some results of these observations are presented in Figures 6(a – d). Figure 6(a) shows the lower-energy (3 – 50 keV) X-ray flux both in the impulsive and post-eruptive phases of the flare. One can see a remarkable increase of the flux in the impulsive phase in the 3 – 6 keV, 6 – 12 keV and 12 – 25 keV bands and weak enhancements of the flux in the 25 – 50 keV band occurred at about 06:46 UT. Reliable records in the 3 – 6 keV and 6 – 12 keV bands show that the flux progressively decreased after 08 UT. So, according to RHESSI and GOES data, the characteristic feature of the related C6.3 flare was a rather slow lower-energy emission increase in the impulsive phase and a slow decrease after the flare peak. This is not typical for most C flares which can be observed on the disk. As to the limb event on 25 January 2007, the X-ray flare features mentioned above are probably due to the fact that the foot points of the northern flare loops were situated behind the solar limb during the X-ray observations. The 195 Å images show that a northern system of loops began to develop at ∼08:25 UT, after the southern one.
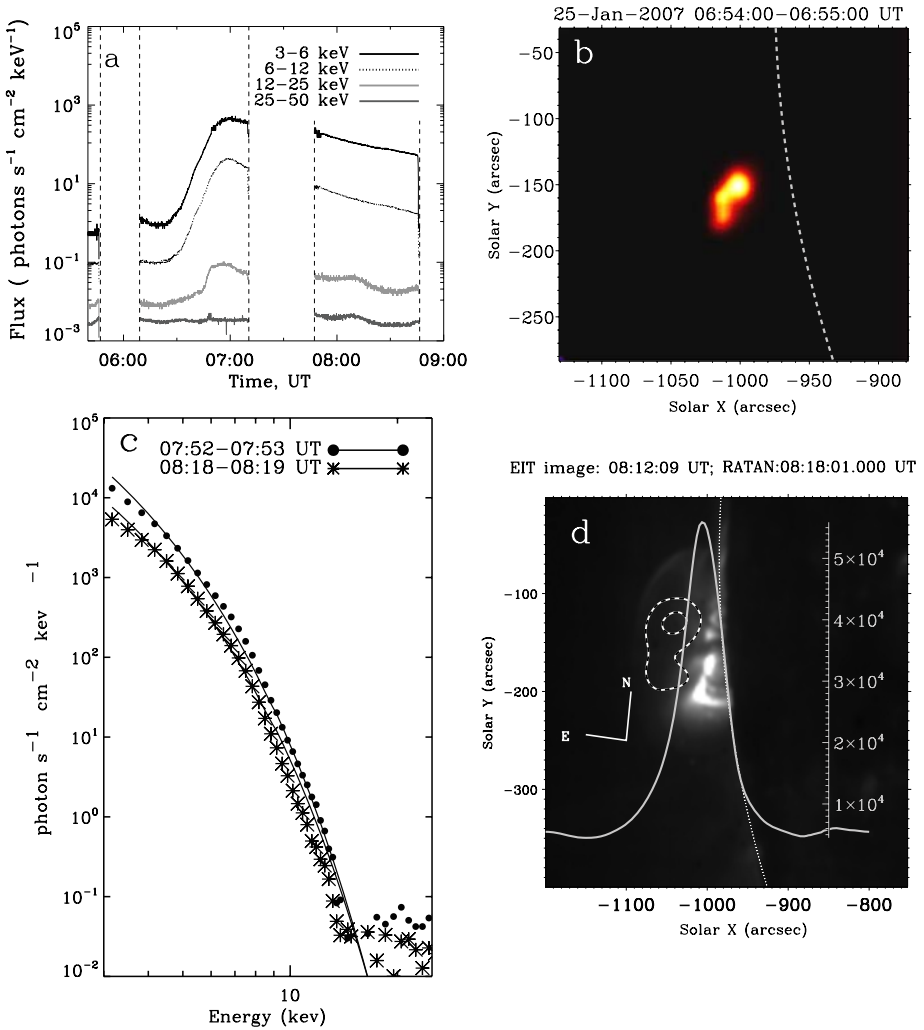
Figure 6 (a) Low energy X-ray flux observed by RHESSI (from top to bottom): 3–6 keV, 6–12 keV, 12–25 keV, 25–50 keV. (b) Reconstructed image of the source in the 6–12 keV channel. (c) Mean HXR photon spectra obtained with RHESSI data. (d) The off-limb radio source extracted from the one-dimensional RATAN-600 solar scan in 2.90 cm (Stokes "*I*") at 08:18:01 UT overlaid on SOHO/EIT 195 Å image at 08:12:09 UT. Dashed lines show the RHESSI image in the 6–12 keV channel (contour levels are 90% and 60% of maximum). The vertical scale shows exceeding emission of the off-limb radio source above the quiet Sun level (in arbitrary units, right scale).

In Figure 6(b) the reconstructed image of the source associated with the flare in the 6–12 keV band at 06:54–06:55 UT is shown. For reconstruction we used the PIXON algorithm (Puetter and Pina, 1994; Schwartz *et al.*, 2002). According to Maltagliati *et al.* (2006), this algorithm provides a better reconstruction of the sources with complex structure than algorithms such as Back Projection, CLEAN, MEM SATO, VIS. We have produced several images of the source in the interval of 06:53–06:57 UT using the PIXON method. The structure of the source varied within this interval. The loop-like shape of the source is clearly

discernible at 06:54 – 06:55 UT. One can see its upper part in Figure 6(b). The height of the source is about 30 000 km above the photosphere.

The spectrum of the X-ray emission for two times (∼08:00 UT) close to the time of the first observation with RATAN-600 is shown in Figure 6(c). The fitting to the thermal model is also shown here by solid lines. One can see that at this time the X-ray emission was thermal. According to RHESSI data, EM = 6.1×10^{47} cm^{-3} and $T_b = 12.8 \times 10^6$ (K) at 07:52 UT.

The position of the X-ray source at 08:17:30 – 08:18:30 UT is shown by contour levels of 90% and 60% of the maximum in Figure 6(d). The off-limb radio source extracted from the one-dimensional RATAN-600 solar scan in 2.90 cm (Stokes "I") at 08:18 UT overlaid on the SOHO/EIT 195 Å image at 08:00 UT is also shown. One can see that the peak intensity of the radio source is co-spatial with the top of 195 Å arcade and the X-ray source adjoins to the northern part of the arcade.

The CME was observed with the Large Angle and Spectrometric Coronagraph (LASCO/C2) on board SOHO from 06:53 UT and with the inner coronagraph (COR1) at the lagging spacecraft STEREO/B (*Behind*), which has registered the CME as a system of loops at a height of 0.7 solar radii above the limb. In Figure 7(a) we show the LASCO/C2 image at 07:31 UT, while Figure 7(b) corresponds to a difference image (between 07:31 and 06:54 UT). The CME looked as a very asymmetric halo, consisting of a system of weak large loops and a compact bright part in the North – East region. According to the SOHO LASCO CME Catalog, the plane-of-the-sky speed from a linear fit to all data points was 1367 km s^{-1}. We pay attention to some features of the North – East part of the CME. Using two calibrated LASCO/C2 images we have estimated the mass of the bright part of the CME visible between PA 40° and 65° in Figures 7(a, b) to be 5×10^{15} g. Such a mass of the CME is typical for powerful CME/flare events.

Attrill *et al.* (2007) proposed for the 25 January 2007 event "a mechanism *via* which CMEs, expanding from a small source region, can naturally become large-scale in the low corona". The morphologies of the CME on 25 January and that of the CME on 24 January were similar (SOHO LASCO CME Catalog). This fact might indicate that both originated from the same magnetic configuration. Some features of CME on 25 January 2007 and those of the post-eruptive arcade development likely due to a filament eruption occurred in this limb event. This filament situated above a presumable neutral line of the photospheric magnetic field was observed along the sunspot group NOAA 10940 crossing the solar disk. Figure 7(c) shows an Hα image of a filament obtained at the Kanzelhöhe Solar Observatory on 27 January 2007 (http://cesar.kso.ac.at/halpha/).

In the radio range the impulsive phase of this rather weak flare was well detected at wavelengths longer than 6 cm up to meter wavelengths (204 MHz). Figure 8 shows the multi-channel time profiles of radio fluxes (Learmonth and IZMIRAN data). At centimeter wavelengths the radio burst was rather weak and its duration was less than 20 min. In decimeter and, especially, in meter wavelengths the emission gradually decreased after the impulsive phase up to 12:00 UT.

Radio data of Learmonth and IZMIRAN show a large group of type III bursts between 06:43 – 06:54 UT followed by the low frequency (<50 MHz) slowly drifting type II burst at 06:45 – 06:50 UT and at about 07:00 UT (see Figure 9(a)). These features of the impulsive phase are well seen in the *Wind*/WAVES space observations (see Figure 9(b)), where type III bursts were detected in the frequency range of 1.075 – 11.975 MHz at 06:54 – 07:06 UT. The weak type II radio burst was also seen in the *Wind*/WAVES observations (from 06:55 UT to 23:30 UT). This burst is described as an "Intermittent weak burst on Fundamental and Harmonic frequencies" in the *Wind*/WAVES catalog. The peak frequency of this burst changed from 10 to 3 MHz during 12 min (see Figure 9(b)).
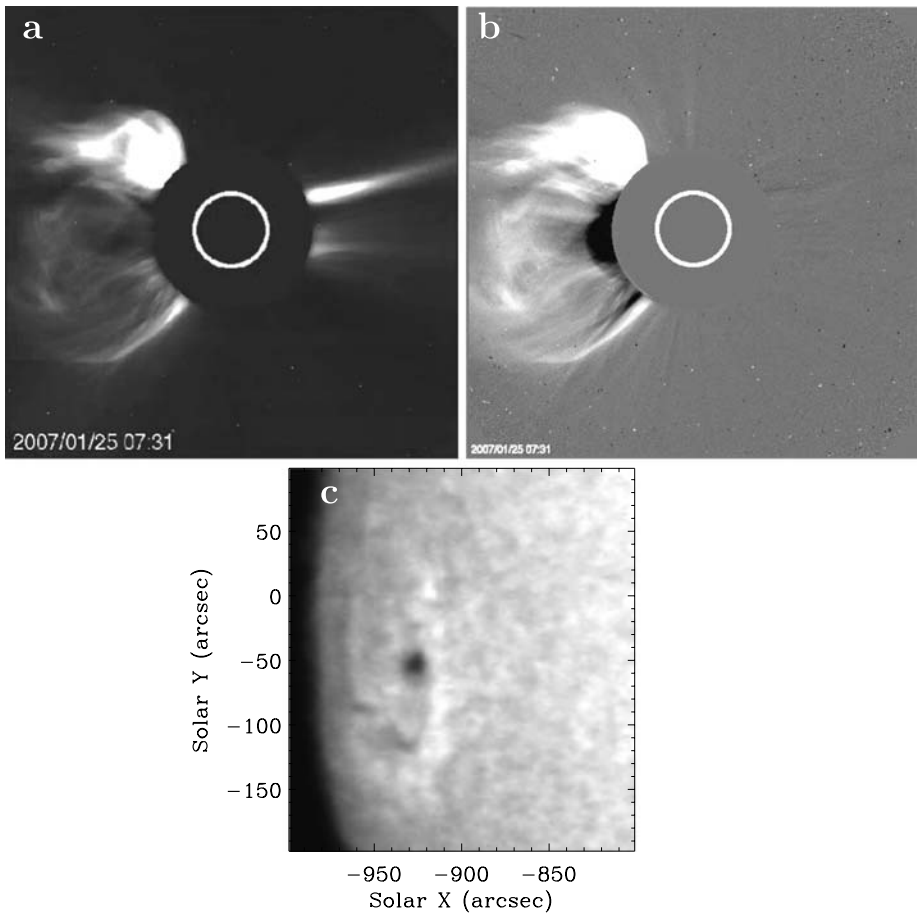
Figure 7 (a) LASCO/C2 CME image at 07:31 UT on 25 January 2007. (b) Difference image between 07:31 UT and 06:54 UT. (c): A section of a Hα image on 27 January 2007 at 08:27 UT (Kanzelhöhe data).

The continuum (noise storm) with many bursts with durations of a few seconds appeared simultaneously with the impulsive phase at frequencies <100 MHz at about 07:00 UT and continued up to 10:30 UT, being more intense at about 07, 08 and 09 UT (see Figure 10). The emission of such groups of bursts in the range of 50–90 MHz drifted downward in frequency. This may be connected with an increase of the height of the radio source above the photosphere (the method and examples of the estimations for the radio source heights are given by Lehtinen *et al.*, 2008). As Figure 10 shows, the continuum was observed also in the high-frequency range of 115–160 MHz and it was clearly discernible in the range of 130–160 MHz at 07:00–07:30 UT. Note that the secondary peak of emission was registered after an impulsive phase at 07:45 UT at 169 and 204 MHz (IZMIRAN) and at 245 MHz (Learmonth) (see Figure 8(a–c)). This peak can be seen in detail in Figure 8(c), where we show a fragment of the time profile (10 s averaging) at frequency 245 MHz (Learmonth) for the time interval 07:30–08:15 UT.

We compare the RATAN-600 microwave data with some features of this event in the meter radio range. RATAN-600 observations covered 3.5 hours (seven observations at inter-
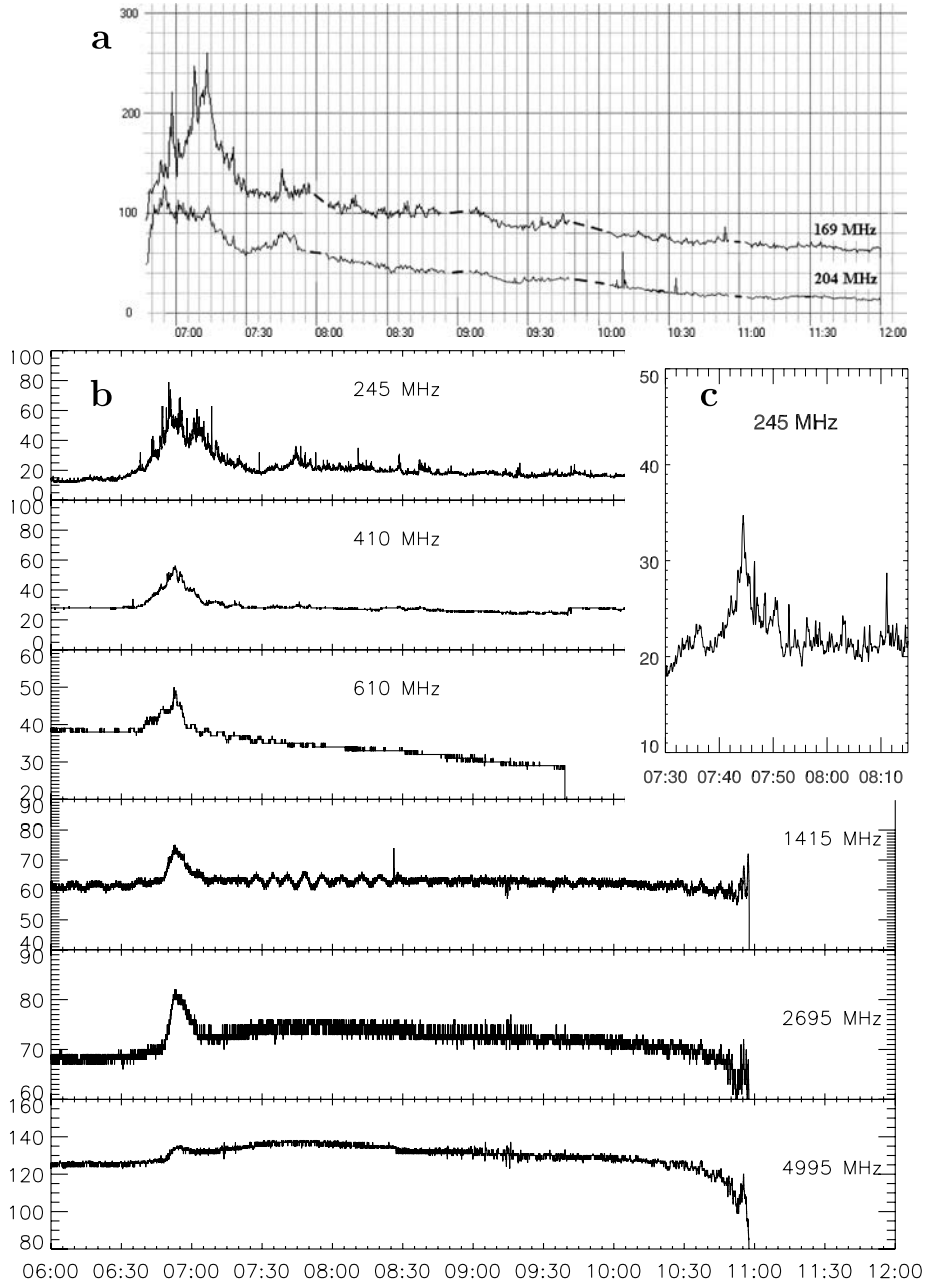
Figure 8 Multi-channel time profiles of radio emission: (a) IZMIRAN data; (b) Learmonth data; (c) fragment of Learmonth time profile at 245 MHz (with 10 s averaging) for 07:30 UT to 08:15 UT.

vals of about 35 min) and coincided with the process of the post-eruptive arcade formation including its early stage. The first two RATAN-600 observations (at 07:44 and 08:18 UT) were made at the initial stage of the arcade development – 30 min and one hour after the
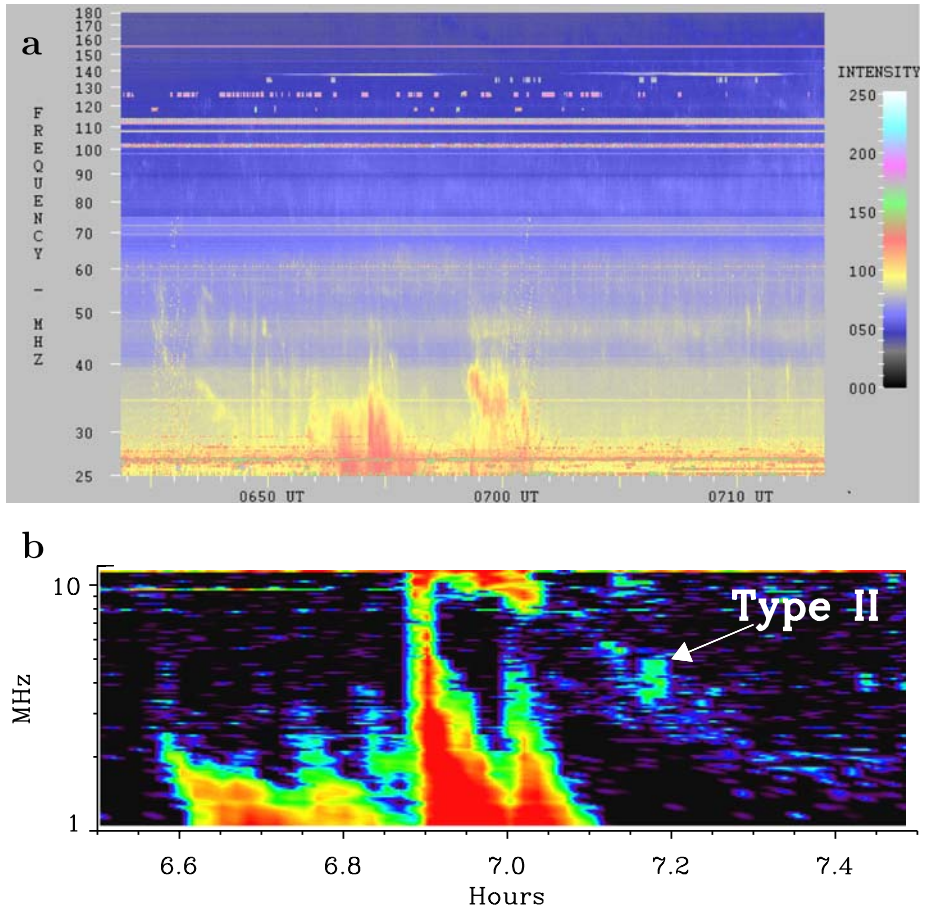
Figure 9 (a) The dynamical spectrum observed during the impulsive phase of the flare on 25 January 2007 (Learmonth data). (b) The radio spectral data observed at the same time for this event (*Wind*/WAVES).

flare peak respectively. As it was mentioned above, just at that time (07:45 UT) a second peak of emission after the impulsive phase was recorded at 245 MHz (Learmonth) as well as at 204 and 169 MHz (IZMIRAN). This is indicative of the presence of a hot plasma and fast particles in the observed region at this time.

The arcade 195 Å images in Figure 4(a, b) show a bright diffuse formation above the flare loop arcade close to the east limb at 07:36 – 07:48 UT. Later, as the flare proceeded, the set of loops ascending above the solar limb during several hours are well seen. The southern part of the arcade appeared first and then the northern one. The RATAN-600 data showed that the peak of the microwave emitting region was co-spatial with the top of the loop structure during the whole period of observation.

The RATAN-600 microwave total flux spectra (see Figure 5) show a great contribution of thermal emission, especially at the initial stage of the arcade formation. Later, as the arcade developed, the thermal contribution considerably decreased. At the same time the radio data at meter wavelengths presented above (see Figure 10) are indicative of non-thermal processes up to 10:30 UT, which is in accordance with the dynamical spectra (Learmonth
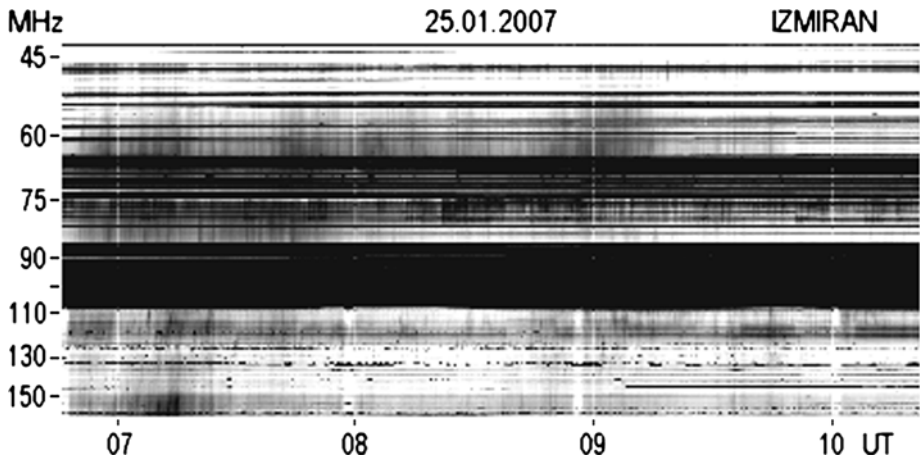
Figure 10 The IZMIRAN spectrum (40 – 160 MHz) shows the noise storm, which starts simultaneously with the flare and is observed in the range of 50 – 80 MHz as groups of bursts around 08 and 09 UT.

data) given in Figure 9(a). The microwave spectra (RATAN-600) confirm that the radio emission during the whole period under consideration was generated both by thermal and non-thermal mechanisms.

4. Discussion

A CME/flare event occurred at the eastern limb on 25 January, 2007. Seven successive multi-wavelength radio observations in the range of 1.8 cm – 5.0 cm were carried out at the RATAN-600 radio telescope starting at the early stage of the post-eruptive arcade formation (30 min after a C6.3 flare peak) and lasting for 3.5 hours. The conditions were favorable to study the off-limb microwave radio source associated with the post-eruptive arcade at different stages of its development. The RATAN-600 data showed that the microwave radio emission of the arcade was rather intense at the initial stage of its formation and considerably decreased later. Its maximum was located at the 195 Å Fe XII loop tops at all stages of the arcade expansion.

The total flux spectrum of the off-limb radio source was practically flat in the range of 1.8 cm – 5.0 cm at the initial stage. This allows us to interpret the microwave emission of the arcade at this stage in terms of bremsstrahlung of an optically thin isothermal source. The spectrum of the soft X-ray source at the loop top, obtained with RHESSI at that time, was also thermal. At the same time, the observational data available in the metric range were indicative of non-thermal processes in the arcade for, at least, three hours after the onset of its formation. This might be indicative of accelerated particles. However, the contribution of non-thermal processes in the microwave and soft X-ray emission at the initial stage of the post-eruptive arcade formation was negligible with respect to stronger thermal emission.

We estimated the plasma parameters in the arcade at the beginning of its formation (30 minutes – one hour after the flare peak) from the first two RATAN-600 observations, and we obtained emission measures EM $= 14.6 \times 10^{48}$ cm^{-3} at 07:44 UT and EM $= 7.5 \times 10^{48}$ cm^{-3} at 08:18 UT. Assuming a volume for the emission region of $V = D^3$, where D is the effective size of the radio source in the direction of scanning, we get the average electron density $N_e = 2.2 \times 10^{10}$ cm^{-3} and $N_e = 1.0 \times 10^{10}$ cm^{-3}, respectively. The

emission measure, obtained for the upper part of the arcade in the range of $3 - 50$ keV from RHESSI data at the same time (07:52 UT) is EM $= 6.1 \times 10^{47}$ cm^{-3} and $T_b = 12.8 \times 10^6$(K). We note that the values of EM, obtained from microwave observations, relate to the plasma in a wide temperature interval. For this reason the emission measure of the hot coronal source in the event on 25 January 2007, as well as in other cases, is less than that of the microwave source. The main conclusion of this paper is the detection of a large amount of hot plasma at the coronal heights at the initial stage of the arcade formation. The temperature of its main part is $3 - 6$ MK, although its lesser part may be hotter.

We note that electron densities were evaluated from the microwave data in the single-temperature approximation for a homogeneous spherically-symmetric source. Electron densities within coronal loops are expected to be higher by a factor of $\sqrt{f}$, where f is a filling factor (typically assumed to be ~ 10 for arcades emitting in soft X-rays). On the other hand, we have used a thermal model ignoring the contribution from a non-thermal mechanism that somewhat decreased the estimated N_e. Anyway, the parameters found are typical of post-eruptive arcades (with the exception of very powerful events) and could be used in estimations of trapping time of accelerated particles in loops, radiative losses of plasma, *etc*.

Observations with the RATAN-600 radio telescope showed that two hours after the flare peak and later the intensity of microwave emission considerably decreased at all frequencies of the operated ranges and the microwave spectra increasingly declined at high frequencies. Taking into account that the degree of polarization did not exceed $10 - 12$ % at wavelengths shorter than 3 cm, one may interpret the microwave emission of the arcade at the late stage as the cyclotron emission of the thermal electrons in a weak magnetic field as well as a small contribution of non-thermal processes (accelerated particles).

We draw attention to the fact that the microwave characteristics of the post-eruptive arcade obtained on 25 January 2007 on the basis of RATAN-600 observations 3.5 hours after a C6.3 flare are similar to those observed with NoRH, SSRT and RATAN-600 on 22 October 2001, $6 - 8$ hours after a M1 flare (Grechnev *et al.*, 2006b). Indeed, in both cases the flux of the microwave source increased with the wavelength: from 1.6 s.f.u. (1.8 cm) to 4.6 s.f.u. (5.0 cm) on 25 January 2007 and from 1.3 s.f.u. (1.9 cm) to 4.5 s.f.u. (3.2 cm) on 22 October 2001. Moreover, the degree of polarization of the microwave emission in both cases did not exceed $10 - 12$ % according to the NoRH and RATAN-600 data.

We have compared our results with those from other events, for example, from the powerful CME/flare event on 21 April 2002 (flare X1.5 class) with a well defined post-eruptive arcade. This event has been studied in different ranges by many authors (see, *e.g.*, Gallagher *et al.*, 2002, 2003; Kundu *et al.*, 2004; Sheeley, Warren, and Wang, 2004; Chernov, 2006). In this event HXR-emission (>50 keV) was detected in the early stage of the eruptive process as well as the non-thermal emission of the compact radio source located low in the corona at the base of the arcade. On 25 January 2007 the hard X-ray emission was not registered, probably because the flare being weaker (class C6.3, GOES) and the source location being different (*i.e.* the onset of the eruptive event was behind the eastern limb). In these two events there were different features in the radio wavelength range. The fine structure was not recorded in IZMIRAN data in the event on 25 January 2007 but it was recorded by the spectropolarimeter of the Huairou station (China) in the range $2.6 - 3.8$ GHz on 21 April 2002, during all the eruptive process (Chernov, 2006). Moreover, fast drifting type III bursts were detected only in the impulsive phase of the event of 25 January 2007 but they were present during the whole event on 21 April 2002 (*Wind*/WAVES).

One can compare the characteristics of the CME and radio bursts associated to eruptive events followed by the formation of a post-eruptive arcade. For example, in the event on 2 June 2003, studied by Pohjolainen (2008) a long-duration stage was absent (GOES data).

The CME (related to a M4.6 GOES class flare) was not a large-scale event according to the SOHO LASCO CME Catalog. The plane-of-the-sky speed from a linear fit to all data points was 980 km s^{-1} and we had a nearly constant velocity. On the contrary, the 25 January 2007 event was a long-duration one (LDE) and a long-lived arcade was observed during more than 6 hours after the impulsive phase related to a C6.3 flare.

Two CMEs, occurring on 9 November 2002, have been studied by Lehtinen *et al.* (2008). The first CME had no long-duration phase. The CME was not a large-scale event, and its plane-of-the-sky speed was 530 km s^{-1}. Only the second CME in this event was a halo (related to an M3.9 flare) and its plane-of-the-sky speed was 1840 km s^{-1}. A bright post-eruptive arcade was observed in the SOHO/EIT Fe XII 195 Å image, but it was not a long-lived one. An EIT wave was observed in the same data. The features of the type II bursts obtained with *Wind*/WAVES were different on 9 November 2002 and on 2 June 2003: an interplanetary type II burst was observed at 14 MHz – 20 kHz on 9 November 2002 (Lehtinen *et al.*, 2008), but it was not registered on 2 June 2003. Note, for comparison, that a weak coronal type II burst was detected on 25 January 2007.

Observations of many CME/flare events show that CMEs and flares are two different manifestations of the same magnetic process in the corona, and they have a strongly coupled relationship but not a cause-effect one (see, *e.g.*, Zhang *et al.*, 2001). Moreover, it was shown that wide ejections and bright large-scale CMEs are usually accompanied by the formation and the presence of a large-scale long-duration arcade (see, *e.g.*, Shakhovskaya, Livshits, and Chertok, 2006). The analysis of the X3 flare of 15 July 2002, given in this paper, illustrates one possibility of the development of post-eruptive processes in events with a powerful impulsive energy release. Here the powerful energy release caused an eruption directed toward the neutral line of the large-scale magnetic field, which was followed by its disturbance. Such a possibility is realized in many powerful events (*e.g.*, on 15 June 1991). Another possibility of the arcade development connected with the filament eruption also does exist. This eruption may occur even outside the active region. These processes affect directly a large-scale magnetic field and cause a large-scale reconstruction of the corona. The flux of X-ray emission in such events is not large in spite of the large area of weak X-ray and Hα ribbons, which appear in some processes.

Both possibilities mentioned above were not realized obviously in the studied event of 25 January 2007, because neither a powerful impulsive energy release was present, nor a large-scale prominence eruption was observed. We draw attention to a bright part of the CME northward of the arcade (Figures 7(a, b)), which probably evolved from the active region near the neutral line of a large-scale magnetic field. Probably, this eruption has appeared in the active region near the neutral line of the large-scale magnetic field. It is interesting to know how a magnetic field emergence and appearance of shear may cause a CME with features such as a direction of the eruption relative to the neutral line, the velocity of the eruption, and the coronal density in the region of the CME formation, which might be favorable for the formation of the long-lived post-eruptive arcades. It is important to study these problems both in observational and in theoretical aspects.

References

Altyntzev, A.T., Grechnev, V.V., Nakajima, H., Fujiki, K., Nishio, M., Prosovetsky, D.V.: 1999, *Astron. Astrophys. Suppl.* **113**, 415.

Attrill, G.D.R., Harra, L.K., van Driel-Gesztelyi, L., Démoulin, P., Wülser, J.-P.: 2007, *Astron. Nachr.* **328**(8), 760.

Borovik, V.N., Gelfreikh, G.B., Bogod, V.M., Korzhavin, A.N., Krüger, A.: 1989, *Solar Phys.* **124**, 157.

Borovik, V.N., Grechnev, V.V., Abramov-Maximov, V.E., Grigorieva, I.Y., Bogod, V.M., Kaltman, T.I., Korzhavin, A.N.: 2007, In: Zaitsev, V.V., Bogod, V.M., Stepanov, A.V. (eds.) *Proc. Conf. on Multiwaves Researches of the Sun*, S.-Petersburg, 370 (in Russian).

Carmichael, H.: 1964, In: Hess, W.N. (ed.) *AAS-NASA Symp. on the Physics of Solar Flares*, NASA, Washington, 451.

Chernov, G.P.: 2006, *Space Sci. Rev.* **127**, 195.

Feldman, U., Seely, J.F., Doschek, G.A., Brown, C.M., Phillips, K.J.H., Lang, J.: 1995, *Astrophys. J.* **446**, 860.

Gallagher, P.T., Dennis, B.R., Krucker, S., Schwartz, R.A., Tolbert, K.: 2002, *Solar Phys.* **210**, 341.

Gallagher, P.T., Lawrence, G.R., Dennis, B.R.: 2003, *Astrophys. J.* **588**, L53.

Gary, G.A., Moore, L.R.: 2004, *Astrophys. J.* **611**, 545.

Gopalswamy, N., Barbieri, L., Cliver, E.W., Lu, G., Plunkett, S.P., Skoug, R.M.: 2005a, *J. Geophys. Res.* **110**, A09S00.

Gopalswamy, N., Yashiro, S., Liu, Y., Michalek, G., Vourlidas, A., Kaiser, M.L., Howard, R.A.: 2005b, *J. Geophys. Res.* **110**, A09S15.

Grechnev, V.V., Zandanov, V.G., Uralov, A.M., Maksimov, V.P., Borovik, V.N., Gelfreikh, G.B., Grigorieva, I.Y., Medar, V.G., Korzhavin, A.N.: 2004, *Solar Phys.* **225**, 379.

Grechnev, V.V., Kuzin, S.V., Urnov, A.M., Zhitnik, I.A., Uralov, A.M., Bogachev, S.A., Livshits, M.A., Bugaenko, O.I., Zandanov, V.G., *et al.*: 2006a, *Solar Syst. Res.* **40**(4), 286.

Grechnev, V.V., Uralov, A.M., Zandanov, V.G., Rudenko, G.V., Borovik, V.N., Grigorieva, I.Y., Slemzin, V.A., Bogachev, S.A., Kuzin, S.V., Zhitnik, I.A., *et al.*: 2006b, *Publ. Astron. Soc. Japan* **58**(1), 55.

Harra, L.K., Démoulin, P., Mandrini, C.H., Matthews, S.A., van Driel-Gesztelyi, L., Culhane, J.L., Fletcher, L.: 2005, *Astron. Astrophys.* **438**, 1099.

Harra-Murnion, L.K., Schmieder, B., van Driel-Gesztelyi, L., Sato, J., Plunkett, S.P., Rudawy, P., Rompolt, B., Akioka, M., Sakao, T., Ichimoto, K.: 1998, *Astron. Astrophys.* **337**, 911.

Hirayama, T.: 1974, *Solar Phys.* **34**, 323.

Ichimoto, K., Sakurai, T.: 1994, Flare Telescope and Norikura Team. In: Sakurai, T., Hirayama, T., Ai, G. (eds.) *Proc. 2nd Japan – China Seminar on Solar Phys.*, NAO, Tokyo, 151.

Kamio, S., Kurokawa, H., Ishi, T.: 2003, *Solar Phys.* **215**, 127.

Kopp, R.A., Pneuman, G.W.: 1976, *Solar Phys.* **50**, 85.

Korol'kov, D.V., Parijskij, Y.N.: 1979, *Sky Tel.* **57**, 324.

Krüger, A., Hildebrandt, J., Urpo, S., Pohjolainen, S.: 1994, In: *Proc. Symp. New Look at the Sun*, Kofu, 259.

Kundu, M.R.: 1972, *Solar Phys.* **25**, 208.

Kundu, M.R., Garaimov, V.I., White, S.M., Krucker, S.: 2004, *Astrophys. J.* **600**, 1052.

Lehtinen, N.J., Pohjolainen, S., Huttunen-Heikinmaa, K., Vainio, R., Valtonen, E., Hillaris, A.E.: 2008, *Solar Phys.* **247**, 151.

Maltagliati, L., Falchi, A., Teriaca, L.: 2006, *Solar Phys.* **235**, 125.

Nindos, A., Alissandrakis, C.E., Gelfreikh, G.B., Borovik, V.N., Korzhavin, A.N., Bogod, V.M.: 1996, *Solar Phys.* **165**, 41.

Pohjolainen, S.: 2008, *Astron. Astrophys.* **483**, 297.

Puetter, R.C., Pina, R.K.: 1994, *Exp. Astron.* **3**, 293.

Schwartz, R.A., Csillaghy, A., Tolbert, A.K., Hurford, G.J., McTierman, J., Zarro, D.: 2002, *Solar Phys.* **210**, 165.

Schwenn, R., Raymond, J.C., Alexander, D., Ciaravella, A., Gopalswamy, N., Howard, R., Hudson, H., Kaufmann, P., Klassen, A., Maia, D., *et al.*: 2006, *Space Sci. Rev.* **123**, 127.

Shakhovskaya, A.N., Livshits, M.A., Chertok, I.M.: 2006, *Astron. Rep.* **50**(12), 1013.

Sheeley, N.R., Warren, H.R., Wang, Y.-M.: 2004, *Astrophys. J.* **616**, 1224.

Sturrock, P.A.: 1966, *Nature* **211**, 695.

Urpo, S., Krüger, A., Hildebrandt, J.: 1986, *Astron. Astrophys.* **163**, 340.
Urpo, S., Teräsranta, H., Krüger, A., Hildebrandt, J., Ruždjak, V.: 1989, *Astron. Nachr.* **310**(6), 423.
Yashiro, S., Michalek, G., Akiyama, S., Gopalswamy, N., Howard, R.A.: 2008, *Astrophys. J.* **873**(2), 1174.
Zhang, J., Dere, K.P., Howard, A.R., Kundu, M.R., White, S.M.: 2001, *Astrophys. J.* **549**(2), 452.
Zhitnik, I.A., Bugaenko, O.I., Ignat'ev, A.P., Krutov, V.V., Kuzin, S.V., Mitrofanov, A.V., Oparin, S.N., Pertsov, A.A., Slemzin, V.A., Stepanov, A.I., *et al.*: 2003, *Mon. Not. Roy. Astron. Soc.* **338**, 67.